

Dephasing enhanced transport in non-equilibrium strongly-correlated quantum systems

J. J. Mendoza-Arenas¹, T. Grujic¹, D. Jaksch^{1,2} and S. R. Clark^{2,1}

¹Clarendon Laboratory, University of Oxford, Parks Road, Oxford OX1 3PU, United Kingdom and

²Centre for Quantum Technologies, National University of Singapore, 3 Science Drive 2, Singapore 117543

(Dated: February 25, 2013)

A key insight from recent studies is that noise, such as dephasing, can improve the efficiency of quantum transport by suppressing coherent single-particle interference effects. However, it is not yet clear whether dephasing can enhance transport in an interacting many-body system. Here we address this question by analysing the transport properties of a boundary driven spinless fermion chain with nearest-neighbour interactions subject to bulk dephasing. The many-body non-equilibrium stationary state is determined using large scale matrix product simulations of the corresponding quantum master equation. We find dephasing enhanced transport only in the strongly interacting regime, where it is shown to induce incoherent transitions bridging the gap between bound dark-states and bands of mobile eigenstates. The generic nature of the effect is illustrated and shown not to depend on the integrability of the model considered. As a result dephasing enhanced transport is expected to persist in more realistic driven systems of strongly-correlated particles.

Introduction – Recently the effects of noise on the efficiency of quantum transport phenomena have been scrutinised intensely by the scientific community. This has been motivated in part by a series of ground-breaking nonlinear spectroscopic experiments on light-harvesting complexes demonstrating surprisingly long-lived quantum coherence during exciton transport, even in a warm and wet environment [1–3]. Yet transport for purely coherent exciton dynamics in such protein pigment networks is highly suppressed due to destructive interference between different propagation pathways. Instead studies revealed that the remarkably high transport efficiency observed (above 95%) in fact emerges in combination with local noise, such as dephasing, which disrupts this interference opening up previously inhibited pathways for transmission [4–7]. Transport properties in such open systems thus not only defy the traditional understanding of when quantum effects should play a significant role, but also challenge the notion that couplings to the environment unconditionally degrade quantum phenomena.

Different effects of dephasing have been studied in networks populated by single particles, in scenarios such as transport through quantum optical systems [8], information transmission [9] and quantum information processing [10]. However, the interplay between noise and strong correlations induced by interactions in a many-body setting is not yet fully understood. In particular a recent experiment [11] with cold-atoms exploring these effects during time-of-flight expansion raises an important question as to whether and how dephasing can enhance transport in an interacting system.

Here we answer this question in the affirmative by considering a concrete example composed of spinless fermions with nearest-neighbour interactions hopping through a tight-binding chain, as depicted in Fig. 6. This model makes an ideal testbed for several reasons. First, it is equivalent to the well studied XXZ spin-1/2 chain [12–14], representing one of the simplest models of strongly-correlated electron systems, and its physics is still not fully understood despite being Bethe ansatz solvable [15]. Second, the transport properties of such low-dimensional interacting quantum systems remains an im-



FIG. 1: Spinless fermions hop with amplitude τ across a chain, subject to a nearest-neighbour density-density interaction of strength Δ , local dephasing at a rate γ , and boundary driving that injects/ejects fermions at a rate proportional to Γ and driving bias f .

portant open problem, exhibiting anomalous features such as ballistic spin transport and unusually high thermal conductivity, reported experimentally in so-called spin-chain materials [16–19]. In addition to solid state systems like chains of coupled quantum dots [20] or molecular wires embedded between electrodes [21], understanding this model is directly relevant to ion-trap [24], coupled-cavity array [25], and cold-atom [11, 22, 23] quantum systems. Of particular relevance are recent seminal experiments that revealed contact and bulk resistivity of cold fermionic atoms flowing within a narrow mesoscopic channel between a pair of reservoirs [26, 27].

Very similar to this cold-atom experiment we consider a chain attached to two unequal Markovian reservoirs at its boundaries providing continuous incoherent driving, along with local dephasing noise along its extension (see Fig. 6) [28–31]. The transport properties of the chain are then found by computing the current-driving characteristics of its non-equilibrium stationary state (NESS). Being a one-dimensional and homogeneous chain, previously studied single-particle interference effects originating from geometry or disorder are absent [5, 6, 32]. Surprisingly, we show that dephasing-enhanced transport nonetheless emerges so long as the interactions are strong enough. In this regime the NESS forms a cooperative many-body quantum state with a long-ranged domain of particles pinned to one boundary strongly suppressing the current, analogous to a Coulomb or Pauli blockade insulator [29]. Even a small dephasing rate induces incoherent transitions between this bound state, preferentially occupied by the driving, and bands of mobile scatter-

ing states. This effect significantly enhances transport, most especially for regimes where the current is otherwise vanishingly small. We isolate the essential conditions for enhancement and demonstrate its generality beyond the integrable system considered. Furthermore, the mechanism described helps explain recent experimental results with cold-atoms where the expansion of a strongly-interacting atomic gas was found to be slow in the absence of noise and substantially increased once noise was added [11].

Model – We study the interacting spinless fermion chain described by the Hamiltonian (taking $\hbar = 1$ throughout)

$$H = \sum_{j=1}^{N-1} \left[\frac{1}{2} \tau (c_j^\dagger c_{j+1} + \text{h.c.}) + \Delta (n_j - \frac{1}{2})(n_{j+1} - \frac{1}{2}) \right], \quad (1)$$

where c_j^\dagger, c_j are standard fermionic creation/annihilation operators for site j , $n_j = c_j^\dagger c_j$ is the associated number operator, and N is the number of sites. In addition to the tight-binding hopping terms, with amplitude τ , this Hamiltonian has a nearest-neighbour density-density interaction $n_j n_{j+1}$ which, depending on the sign of its strength Δ , either penalizes ($\Delta > 0$) or promotes ($\Delta < 0$) the adjacency of fermions. We take $\tau = 1$ to set the energy scale to which all other quantities are measured. The dynamics of the system is described by a Lindblad quantum master equation [33]

$$\frac{d\rho}{dt} = -i[H, \rho] + \mathcal{L}(\rho), \quad (2)$$

where ρ is the density matrix of the chain, and \mathcal{L} is the dissipator describing the coupling to the Markovian reservoirs. In Lindblad form the dissipator can be expressed as $\mathcal{L}(\rho) = \sum_k (L_k \rho L_k^\dagger - \frac{1}{2} \{L_k^\dagger L_k, \rho\})$, where $\{.,.\}$ is the anti-commutator and the sum is over a set of jump operators L_k . We consider a dissipator that splits into three parts $\mathcal{L} = \mathcal{L}_L + \mathcal{L}_d + \mathcal{L}_R$. Here \mathcal{L}_L and \mathcal{L}_R describe the coupling to external particle reservoirs at the left and right boundaries, respectively, each with two jump operators $L_{L,R}^\pm = \sqrt{\Gamma(1 \mp f)/2} c_{1,N}$ and $L_{L,R}^\mp = \sqrt{\Gamma(1 \pm f)/2} c_{1,N}^\dagger$, where Γ is the coupling strength, identical for both reservoirs, and $0 \leq f \leq 1$ is the driving bias [29]. We consider moderate coupling $\Gamma = 1$ throughout this paper [34]. The effect of the driving is to force the system far from equilibrium thereby giving a quantum analogue of the well studied classical exclusion stochastic model [35, 36]. As depicted in Fig. 6 it is composed of two processes: *forward pumping* creating particles at the left edge and removing them at the right, and *backwards pumping* doing the opposite. When $f = 0$ these processes have equal strength and so cancel exactly, resulting in the stationary solution $\rho = \mathbb{1}/2^N$ to Eq. (2) with no net current, irrespective of Δ [37]. For $f > 0$ the bias favours forward pumping raising the possibility of a NESS possessing a finite current. The remaining contribution \mathcal{L}_d accounts for bulk dephasing in the chain and is described by a jump operator $L_j^d = \sqrt{\gamma}(1 - 2n_j)$ for each site $j = 1, \dots, N$ with a uniform dephasing rate γ .

By directly simulating Eq. (2) and taking the long time limit, the state $\rho(t)$ converges to the time-independent NESS

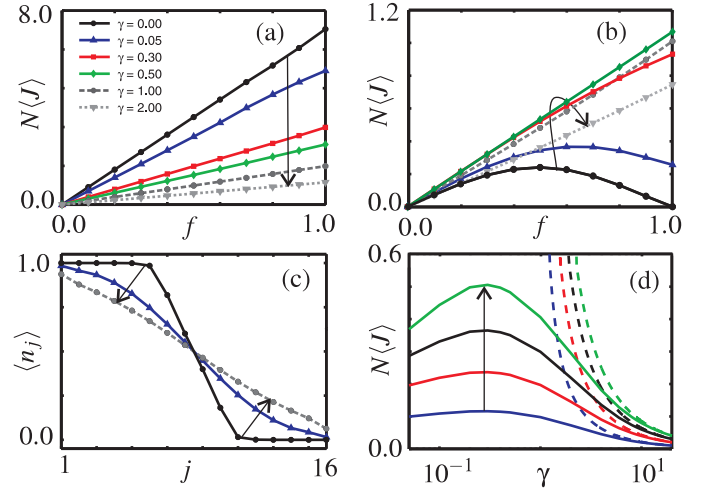


FIG. 2: (a) The current-driving profiles in the weakly-interacting regime $\Delta = 0.5$ for increasing (as indicated by the arrow) dephasing rates γ and $N = 16$. (b) Identical plot to (a) but in the strongly-interacting regime $\Delta = 2$. (c) The density $\langle n_j \rangle$ of the system when $\Delta = 2$, $f = 1$, and $N = 16$, corresponding to $\gamma = 0, 0.05, 1.00$. (d) The current as a function of γ for driving biases $f = 0.1, 0.2, 0.3$ and 0.4 (from bottom to top curve) with $\Delta = 2$, and $N = 40$. The dashed lines correspond to $\langle J \rangle_{\Delta=0}$ the non-interacting analytic result [44, 45].

of the system. A solution can be computed efficiently in a controlled way and accounting for significant many-body correlations by applying the time evolving block decimation (TEBD) algorithm [38, 39] to a matrix product operator description of $\rho(t)$. This highly compact representation enables the efficient evaluation of relevant expectation values and makes accessible much larger system sizes than exact diagonalization or Monte Carlo approaches [40–42]. Moreover TEBD can be applied effectively over a large parameter range allowing us to examine the properties of the system as a function of f beyond the $f \ll 1$ linear response regime [43]. The transport properties are found by computing the current crossing site j from the operator $J_j = i(c_j^\dagger c_{j+1} - \text{h.c.})$. In the NESS the current $\langle J_j \rangle = \langle J \rangle$ is homogeneous throughout the system.

Dephasing enhanced transport – It is known that in the weakly interacting regime $|\Delta| < 1$, in the absence of dephasing, the system is an ideal ballistic conductor for any driving f , with a nearly flat density $\langle n_j \rangle$ and a current $\langle J \rangle \propto f$ which is independent of N [29, 46]. The introduction of dephasing has been shown to induce diffusive transport, where $\langle n_j \rangle$ instead features a constant gradient and $\langle J \rangle \propto f/N$, characteristic of an Ohmic conductor [32, 44]. In either case the maximum current through the chain occurs at maximal bias $f = 1$, where only forward pumping is present, as might be intuitively expected. In the non-interacting limit $\Delta = 0$ it has been proven rigorously that a homogeneous chain cannot exhibit any dephasing enhanced transport [44, 47]; this behaviour was also suggested for weakly-interacting systems where $|\Delta| < 1$ [32]. In Fig. 7(a) a complete picture of the latter result is presented. Specifically, for $\Delta = 0.5$ the reported current-driving profiles

show that dephasing monotonically degrades the current for any driving, confirming that this behaviour persists even in the presence of weak interactions. Thus, the present work focuses on the strongly interacting regime $|\Delta| > 1$.

In the absence of dephasing, and for weak driving $f \ll 1$, transport was found [46] to be diffusive when $|\Delta| > 1$, a controversial finding given that the integrability of the system was initially conjectured to lead to ballistic transport [48]. However, for strong driving $f \rightarrow 1$ it was discovered [29, 49] that the NESS exhibits a particle domain at the left edge of the chain, e.g. dominated by the configuration $|11 \dots 10 \dots 00\rangle$, irrespective of the sign of Δ . This strongly suppresses the current as $\langle J \rangle \propto \exp(-N)$, characteristic of an insulator. Consequently, the current $\langle J \rangle$ at $\gamma = 0$ exhibits non-linear behaviour with the driving f , leading to an effect known as negative differential conductivity (NDC) where increasing the driving eventually decreases the current [29, 49]. In Fig. 7(b) the $\gamma = 0$ curve shows that this causes a near complete suppression at $f = 1$ for $\Delta = 2$. Consequently, in the strongly interacting regime the system presents the intriguing property that more current flows at an intermediate bias $f < 1$ where some backward pumping is present.

The main result of this work is that for $|\Delta| > 1$ the presence of a small bulk dephasing can significantly enhance the current. This striking behaviour is illustrated for $\Delta = 2$ in Fig. 7(b) where dephasing up to a moderate rate $\gamma \approx 0.5$ is seen to increase the current. This elevation in the current is shown to occur for any $f > 0$, however, it is not uniform in f resulting in the current-driving profile changing with γ . Specifically, around $\gamma \approx 0.3$ the NDC effect is lost and further increases in γ yield a linear profile in f , resembling a diffusive conductor (see Supplementary Material). This indicates that the most dramatic enhancement of the current occurs for strong driving biases $f \sim 1$, where the system changes from being insulating at $\gamma = 0$ to yielding the maximal current once $\gamma > 0.3$. In Fig. 7(c) this change at $f = 1$ is shown to be coincident with the breakdown of the particle domain at the left boundary into a near linear density profile even for small dephasing rates. In this regime dephasing therefore induces not just quantitative increases in the current, but rather causes a major qualitative change in the behaviour of the system.

For a given f there is an optimal dephasing rate γ_{opt} , beyond which the current is degraded by dephasing. This is illustrated in Fig. 7(d), where it is shown that both the maximum enhancement of the current and γ_{opt} increase with f . While for a weak driving $f = 0.1$ the current enhancement at its γ_{opt} is 37% relative to $\gamma = 0$, for $f = 1$ the enhancement is $\approx 10^7$. For $\gamma > \gamma_{\text{opt}}$ the current is reduced because the \mathcal{L}_d contribution to Eq. (2) dominates over the coherent hopping terms and freezes out the dynamics by the Zeno effect [33]. In fact for increasingly large dephasing rates the interaction becomes increasingly irrelevant, as demonstrated in Fig. 7(d) by the convergence of the NESS current to the exact $\Delta = 0$ solution with dephasing $\langle J \rangle_{\Delta=0} = -2f/[(\Gamma/4) + (4/\Gamma) + (N-1)\gamma]$ [44, 45].

Enhancement mechanism – The origin of the dephasing enhanced transport in the strongly-interacting regime is inti-

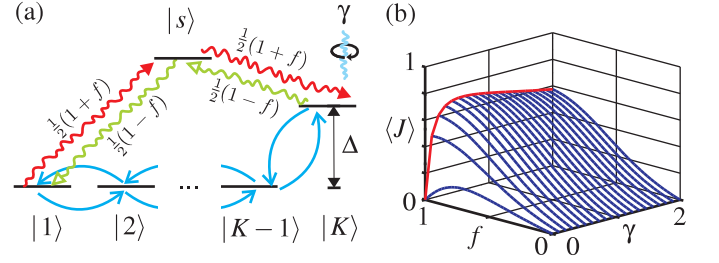


FIG. 3: (a) The toy model composed of states $|1\rangle, \dots, |K\rangle$ coupled coherently to their neighbours and with incoherent driving, via an auxiliary state $|s\rangle$, between states $|1\rangle \leftrightarrow |K\rangle$. Crucially state $|K\rangle$ is elevated in energy by Δ . See Supplementary Material for precise definitions of the model. (b) The current-driving profiles of the toy-model as a function of γ with $\Delta = 2$ and $K = 20$.

mately connected to the appearance of an insulating NESS at $f = 1$. This is most easily revealed by examining the very strongly-interacting limit $|\Delta| \gg 1$ with totally biased driving $f = 1$. Consistent with the numerical findings above, the NESS in this extreme limit is insulating for two reasons: (i) when $|\Delta| \gg 1$ there exists an eigenstate $|\Psi_D(n)\rangle$ of H for each number sector n , which is a bound state energetically separated from other eigenstates; as $n \rightarrow N/2$ it becomes exponentially close, with increasing N , to being a dark state of $f = 1$ driving; (ii) the ergodic nature of the driving and coherent dynamics results in the unique NESS being well approximated by a statistical mixture of $\rho = \sum_{n=0}^N p_n |\Psi_D(n)\rangle \langle \Psi_D(n)|$, with the probability p_n exponentially peaked at $n = N/2$ half-filled domain. The formation of an insulating NESS thus arises due to an interplay between the nature of the boundary driving and the eigenstructure of the chain Hamiltonian. In the Supplementary Material we show (i) and (ii) by examining the structure of the driving and coherent hybridisation of the n particle boundary configuration $|B_n\rangle = |11 \dots 10 \dots 00\rangle$ that forms $|\Psi_D(n)\rangle$. Crucially, bulk dephasing induces energy dissipation at a rate $dE_\gamma/dt = -2\gamma \sum_j \langle c_j^\dagger c_{j+1} + \text{h.c.} \rangle$ proportional to the kinetic energy of the state. As a result dephasing incoherently bridges the spectral gap between $|\Psi_D(n)\rangle$ and mobile bands of scattering states, thereby dramatically enhancing the current as population escapes the dark state.

The effect outlined is captured concretely by a simple toy-model, depicted in Fig. 8(a). The model comprises of states $|1\rangle, |2\rangle, \dots, |K-1\rangle, |K\rangle$, for some size K , with coherent coupling between neighbouring states. The state $|K\rangle$ is elevated in energy by Δ above the rest, analogous to the configuration $|B_n\rangle$; the other states correspond to breakaway configurations like $|11 \dots 1010 \dots 00\rangle$. This yields a mobile band of $K-1$ eigenstates and a single bound state of the form $|\Psi_D\rangle \approx \sum_{k=0}^{K-1} |2\Delta|^{-k} |K-k\rangle$, irrespective of the sign of Δ . Via an auxiliary state $|s\rangle$, modelling another particle number sector, incoherent driving is included between states $|1\rangle$ and $|K\rangle$ with an identical f dependence as the full system (see Supplementary Material for details). Dephasing is also introduced which scrambles the phase between $|K\rangle$ and all other

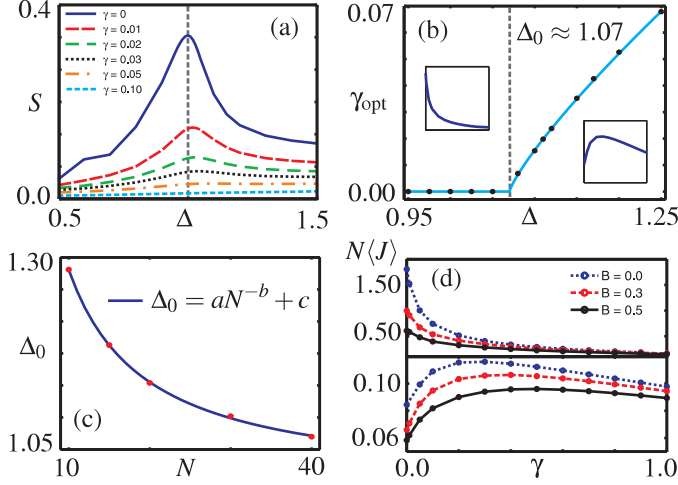


FIG. 4: For $f = 0.1$ and $N = 40$: (a) The half-chain entropy S as a function of Δ for different γ 's, and (b) The optimal dephasing rate γ_{opt} as a function of Δ . The circles indicate TEBD results, and the solid line corresponds to the fitted function $\gamma_{\text{opt}} \propto (\Delta - \Delta_0)^\beta$, with $\beta = 0.819$ and $\Delta_0 = 1.07$. The inset plots show the generic behaviour of $\langle J \rangle$ with γ above and below Δ_0 . (c) The scaling of Δ_0 with N along with the fitted power-law shown where $a = 3.906$, $b = 1.066$ and $c = 0.995$. (d) The current for several staggered potential strengths B with $\Delta = 0.5$ (upper panel) and $\Delta = 2.0$ (lower panel).

states. Now since the amplitude for $|1\rangle$ in $|\Psi_D\rangle$ scales as $|\Delta|^{1-K}$ it is exponentially close to being a dark state of $f = 1$ driving. Moreover, as $f = 1$ driving pumps into the majority component $|K\rangle$ of $|\Psi_D\rangle$, it leads to an insulating NESS at the extremal point $f = 1$ and $\gamma = 0$. The current-driving profile is shown as a function of f and γ in Fig. 8(b), and is seen to reproduce both NDC and dephasing enhancement of the strongly-interacting regime of the full system. The toy-model thus reveals that this behaviour is entirely a consequence of the insulator at $f = 1$ and $\gamma = 0$. Moreover, it also shows that same physics underpins the NDC effect as dephasing enhancement. When $f = 1$ and $\gamma > 0$ dephasing induces incoherent transitions to the mobile band. Similarly for $\gamma = 0$ and $f < 1$ the leading order effect of the weak backward pumping process $|s\rangle \leftarrow |K\rangle$, followed rapidly by the stronger forward pumping process $|s\rangle \rightarrow |K\rangle$, is to decohere $|\Psi_D\rangle$.

Signature of a non-equilibrium phase transition – The toy-model is only valid for $|\Delta| \gg 1$ and predicts NDC for any $|\Delta| > 0$. In the non-interacting $\Delta = 0$ limit the exact solution $\langle J \rangle_{\Delta=0}$ indicates that dephasing acts only to degrade the current. However, numerical results presented in Fig. 7(a) already indicate that dephasing-degrading behaviour persists with weak interactions [32]. This suggests that between the regimes $|\Delta| \ll 1$ and $|\Delta| \gg 1$ a cross-over in the response of the system to dephasing emerges. The point $|\Delta| = 1$ is of particular significance since at zero-temperature it separates the equilibrium phases of the underlying spinless fermion Hamiltonian, marking the opening of a gap above the ground state, and more generally divides a continuous eigen-spectrum for

$|\Delta| < 1$ from one with numerous gaps for $|\Delta| > 1$ [50, 51]. In the driven system it was previously observed that $|\Delta| \approx 1$ also separates ballistic and diffusive transport regimes for weak driving [29], however directly linking these equilibrium and non-equilibrium properties can be misleading [53].

For $\gamma = 0$, studies have attempted to identify the non-equilibrium regimes by examining two-point correlations, such as $C_{ij} = \langle n_i n_j \rangle - \langle n_i \rangle \langle n_j \rangle$. The strongly-interacting regime was found to retain correlations extending over a fraction of the entire system as its size increases, while the weakly-interacting regime does not, with a sharp cross-over found at $\Delta_c \approx 0.91$ [52]. Here we refine this signature by adopting a more general measure of correlations. Specifically, we compute the entropy $S = -\sum_\alpha \lambda_\alpha^2 \log_2 \lambda_\alpha^2$ of the Schmidt coefficients λ_α arising when the full NESS density operator ρ is factorized into two half-chains as $\rho = \sum_\alpha \lambda_\alpha O_\alpha^A O_\alpha^B$ [38, 46, 55]. The entropy S quantifies both the quantum and classical correlations between the two halves of the chain and is readily accessible within the matrix product operator description used in TEBD numerics. For zero dephasing Fig. 9(a) shows that S features a peak at $\Delta \approx 1$, indicating that a significant elevation in correlations occurs as the NESS reorganises itself across the expected non-equilibrium phase transition between ballistic and diffusive transport there.

For finite dephasing the entropy S monotonically decreases with γ , but interestingly, the peak is maintained for moderate rates shifting slightly to larger Δ . Similar to C_{ij} this distinguishing feature in S is progressively washed out as the system becomes diffusive for all Δ with dephasing [32, 44, 45] (see also Supplementary Material). Despite this, dephasing in fact offers an alternative and clear signature of this underlying non-equilibrium phase transition. In Fig. 9(b) we show the optimal dephasing rate γ_{opt} for weak driving as a function of Δ , for $N = 40$. A threshold of $\Delta_0 \approx 1.07$ is apparent where for $\Delta < \Delta_0$, $\gamma_{\text{opt}} = 0$, indicating dephasing-degrading transport, while for $\Delta > \Delta_0$, γ_{opt} is non-zero and increases monotonically with Δ , indicating dephasing-enhanced transport. The value of Δ_0 is size-dependent, and a scaling analysis shown in Fig. 9(c) demonstrates that, to good approximation, the isotropic point $\Delta = 1$ separates these regimes in the thermodynamic limit. The abrupt on-set of dephasing enhancement therefore occurs when the many-body strong correlations are largest.

Conclusions – We have presented a study of the effects of dephasing on the transport properties in a boundary driven one-dimensional interacting spinless fermion chain. The appearance of a cooperative many-body NESS exhibiting NDC provides a previously unexplored form of dephasing enhanced transport, distinct in origin from earlier examples in non-interacting systems. Using a toy model we isolated the minimum requirements for observing NDC and dephasing enhanced transport in a strongly-interacting system. The effect is also unrelated to integrability [56], suggesting that our findings it will also apply in related, more realistic models of strongly-correlated electrons such as the $t - J$ or Hubbard models, and in heat transport [54]. Moreover, tantalising signs of dephasing energy dissipation from bound states predicted

here have already been observed in a recent cold-atom experiment [11]. Finally, the prospects of verifying more directly both NDC and dephasing enhancement with cold-atoms seems promising [26, 27].

J. J. M.-A. acknowledges Departamento Administrativo de Ciencia, Tecnología e Innovación Colciencias for economic support. D.J. and S.R.C. thank the National Research Foundation and the Ministry of Education of Singapore for support.

-
- [1] G. S. Engel, T. R. Calhoun, E. L. Read, T.-K. Ahn, T. Mancal, Y.-C. Cheng, R. E. Blankenship and G. R. Fleming, *Nature* **446**, 782 (2007).
- [2] H. Lee, Y.-C. Cheng, and G. R. Fleming, *Science* **316**, 1462 (2007).
- [3] E. Collini, C. Y. Wong, K. E. Wilk, P. M. G. Curmi, P. Brumer, and G. D. Scholes, *Nature* **463**, 644 (2010).
- [4] M. Mohseni, P. Rebentrost, S. Lloyd and A. Aspuru-Guzik, *J. Chem. Phys.* **129**, 174106 (2008).
- [5] F. Caruso, A. W. Chin, A. Datta, S. F. Huelga and M. B. Plenio, *J. Chem. Phys.* **131**, 105106 (2009).
- [6] P. Rebentrost, M. Mohseni, I. Kassal, S. Lloyd and A. Aspuru-Guzik, *New J. Phys.* **11**, 033003 (2009).
- [7] A. W. Chin, A. Datta, F. Caruso, S. F. Huelga and M. B. Plenio, *New J. Phys.* **12**, 065002 (2010).
- [8] F. Caruso, N. Spagnolo, C. Vitelli, F. Sciarrino and M. B. Plenio, *Phys. Rev. A* **83**, 013811 (2011).
- [9] F. Caruso, S. F. Huelga and M. B. Plenio, *Phys. Rev. Lett.* **105**, 190501 (2010).
- [10] A. Bermudez, T. Schaetz and M. B. Plenio, arXiv: 1210.2860v2 (2012).
- [11] C. D’Errico, M. Moratti, E. Lucioni, L. Tanzi, B. Deissler, M. Inguscio, G. Modugno, M.B. Plenio and F. Caruso, arXiv:1204.1313 (2012).
- [12] D. Gobert, C. Kollath, U. Schollwöck and G. Schütz, *Phys. Rev. E* **71**, 036102 (2005).
- [13] S. Langer, F. Heidrich-Meisner, J. Gemmer, I. P. McCulloch and U. Schollwöck, *Phys. Rev. B* **79**, 214409 (2009).
- [14] S. Keßler, A. Holzner, I. P. McCulloch, J. von Delft and F. Marquardt, *Phys. Rev. A* **85**, 011605(R) (2012).
- [15] H. Bethe, *Z. Phys. A* **71**, 205 (1931).
- [16] A. V. Sologubenko, T. Lorenz, H. R. Ott and A. Freimuth, *J. Low Temp. Phys.* **147**, 387 (2007).
- [17] F. Heidrich-Meisner, A. Honecker and W. Brenig, *Eur. Phys. J. Special Topics* **151**, 135 (2007).
- [18] N. Hlubek, P. Ribeiro, R. Saint-Martin, A. Revcolevschi, G. Roth, G. Behr, G. Büchner and C. Hess, *Phys. Rev. B* **81**, 020405(R) (2010).
- [19] O. Janson, A. A. Tsirlin and H. Rosner, *Phys. Rev. B* **82**, 184410 (2010).
- [20] R. Hanson, L. P. Kouwenhoven, J. R. Petta, S. Tarucha and L. M. K. Vandersypen, *Rev. Mod. Phys.* **79**, 1217 (2007).
- [21] J. C. Cuevas and E. Scheer, *Molecular Electronics: An introduction to Theory and Experiment* (World Scientific, 2010).
- [22] S. Trotzky, P. Cheinet, S. Fölling, M. Feld, U. Schnorrberger, A. M. Rey, A. Polkovnikov, E. A. Demler, M. D. Lukin, and I. Bloch, *Science* **319**, 295 (2008).
- [23] J. Simon, W. S. Bakr, R. Ma, M. E. Tai, P. M. Preiss, and M. Greiner, *Nature* **472**, 307 (2011).
- [24] J. T. Barreiro, M. Müller, P. Schindler, D. Nigg, T. Monz, M. Chwalla, M. Hennrich, C. F. Roos, P. Zoller, and R. Blatt, *Nature* **470**, 486 (2011).
- [25] A. Kay and D. G. Angelakis, *EPL (Europhysics Letters)* **84**, 20001 (2008).
- [26] J.-P. Brantut, J. Meineke, D. Stadler, S. Krinner, and T. Esslinger, *Science* **337**, 1069 (2012).
- [27] D. Stadler, S. Krinner, J. Meineke, J.-P. Brantut, and T. Esslinger, *Nature* **491**, 736 (2012).
- [28] G. Benenti, G. Casati, T. Prosen and D. Rossini, *EPL (Europhysics Letters)* **85**, 37001 (2009).
- [29] G. Benenti, G. Casati, T. Prosen, D. Rossini and M. Žnidarič, *Phys. Rev. B* **80**, 35110 (2009).
- [30] T. Prosen, *Phys. Rev. Lett.* **106**, 217206 (2011).
- [31] M. Žnidarič, *Phys. Rev. Lett.* **106**, 220601 (2011).
- [32] M. Žnidarič, *New J. Phys.* **12**, 043001 (2010).
- [33] H.-P. Breuer and P. Petruccione, *The theory of open quantum systems* (Oxford University Press, 2002).
- [34] The validity of the master equation description in this regime was established in earlier works [28–31].
- [35] B. Derrida, *Phys. Rep.* **301**, 65 (1998).
- [36] O. Golinelli and K. Mallick, *J. Phys. A* **39**, 12679 (2006).
- [37] D. Burgarth and V. Giovannetti, *Phys. Rev. Lett.* **99**, 100501 (2007).
- [38] M. Zwolek and G. Vidal, *Phys. Rev. Lett.* **93**, 207205 (2004).
- [39] S. Al-Assam, S. R. Clark, D. Jaksch and TNT Development Team, TNT Library alpha version (2012), <http://www.tensornetworktheory.org>.
- [40] M. Michel, O. Hess, H. Wichterich and J. Gemmer, *Phys. Rev. B* **77**, 104303 (2008).
- [41] J. Wu and M. Berciu, *Phys. Rev. B* **83**, 214416 (2011).
- [42] V. Popkov, M. Salerno, and G. M. Schütz, *Phys. Rev. E* **85**, 031137 (2012).
- [43] Simulations at strongly biased drivings $f \rightarrow 1$ and small dephasing rates is extremely demanding due to the formation of an insulating NESS central to this work. This limits the system sizes accessible.
- [44] M. Žnidarič, *J. Stat. Mech.* L05002 (2010).
- [45] M. Žnidarič, *Phys. Rev. E* **83**, 011108 (2011).
- [46] T. Prosen and M. Žnidarič, *J. Stat. Mech.* P02035 (2009).
- [47] M. B. Plenio and S. F. Huelga, *New J. Phys.* **10**, 113019 (2008).
- [48] X. Zotos, F. Naef, and P. Prelovšek, *Phys. Rev. B* **55**, 11029 (1997).
- [49] T. Prosen, *Phys. Rev. Lett.* **107**, 137201 (2011).
- [50] B. Sutherland, *Beautiful Models. 70 Years of Exactly Solved Quantum Many-Body Problems* (World Scientific, 2005).
- [51] M. Takahashi, *Thermodynamics of One-Dimensional Solvable Models* (Cambridge University Press, 1999).
- [52] T. Prosen and M. Žnidarič, *Phys. Rev. Lett.* **105**, 060603 (2010).
- [53] The transport phenomena outlined here occur irrespective of the sign of Δ , meaning that it can involve highly excited eigenstates of H , and are also insensitive to the presence of a uniform potential $\propto \sum_{j=1}^N n_j$ [54], in contrast to the equilibrium transition.
- [54] J. J. Mendoza-Arenas, S. Al-Assam, S. R. Clark, and D. Jaksch, *in preparation*.
- [55] M. Žnidarič, T. Prosen and I. Pižorn, *Phys. Rev. A* **78**, 022103 (2008).
- [56] Integrability of the Hamiltonian in Eq. (1) can be broken by adding a staggered potential $B \sum_{j=1}^N (-1)^j n_j$. For $\gamma = 0$ this has the effect of turning the system into a diffusive conductor in the gapless regime $|\Delta| < 1$ for any driving, while not affecting the existence of NDC at large drivings for $|\Delta| > 1$ [29]. In Fig. 9(d) we confirm, for several field strengths B , that dephasing-enhanced transport occurs for $|\Delta| > 1$ only, while for $|\Delta| < 1$ dephasing monotonically decreases the current.

Supplementary Material: “Dephasing enhanced transport in non-equilibrium strongly-correlated quantum systems”

In these appendices we consider in more detail a number of points discussed in the main text. Specifically, in Sec. we provide evidence that for a strongly interacting regime $|\Delta| \gg 1$ at maximal bias $f = 1$ the transport becomes diffusive in the large dephasing limit $\gamma > 1$. This is followed in Sec. with an analysis of the structure of driving at $f = 1$ between configuration states. Using this we demonstrate that a dark state exists in the limit $|\Delta| \gg 1$ and we characterise it and the properties of the non-equilibrium stationary state (NESS) using perturbative arguments. In Sec. the essential features of the strongly interacting limit are reduced down into a toy-model which is seen to exhibit a current-driving profile very similar to the full spinless fermion system. The simplicity of the model allows an analytic study of its properties and complements the results given in the main text. Finally, in Sec. the effects of dephasing on the two-point correlations in the full system are outlined.

DIFFUSIVE TRANSPORT WHEN $|\Delta| > 1$ WITH $f = 1$ AND $\gamma > 0$

In the strongly-interacting regime dephasing is seen to modify the current-driving profile from an NDC curve to being linear in f . At $f = 1$ this is also coincident with the breakdown of the particle domain pinned to the left boundary giving way to a linear density profile $\langle n_j \rangle$. Both these features suggest that dephasing alters the strongly-interacting maximally biased regime from being insulating to diffusive. Here we present scaling evidence to prove this claim.

A diffusive current fulfills the usual diffusion equation $\langle J \rangle = \kappa \nabla \langle n_j \rangle$, where κ is the conductivity. Given that when $\gamma > 0$ we observe that $\langle n_j \rangle$ is linear in j everywhere but the boundary sites, its gradient simplifies to

$$\nabla \langle n_j \rangle = \frac{\langle n_{N-1} \rangle - \langle n_2 \rangle}{N-3} = \frac{\Delta n}{N-3}, \quad (1)$$

where Δn is the density difference between opposite ends of the system (after discarding the boundary sites). This indicates that a signature of diffusive transport will be a scaling

$$\frac{\langle J \rangle}{\Delta n} \propto \frac{1}{N-3}. \quad (2)$$

In Fig. 5 results are presented for the $\langle J \rangle / \Delta n$ at $f = 1$ with $\Delta = 2$ as a function of the system size up to $N = 100$ sites with dephasing rates $\gamma = 0.5$ and $\gamma = 1.0$. Also plotted are power-law fittings for each γ which are seen to accurately model the data. These show that the decay of current with N is subdiffusive, decaying slower than $1/(N-3)$, for $\gamma = 0.5$ but has approached diffusive behaviour once $\gamma = 1.0$.

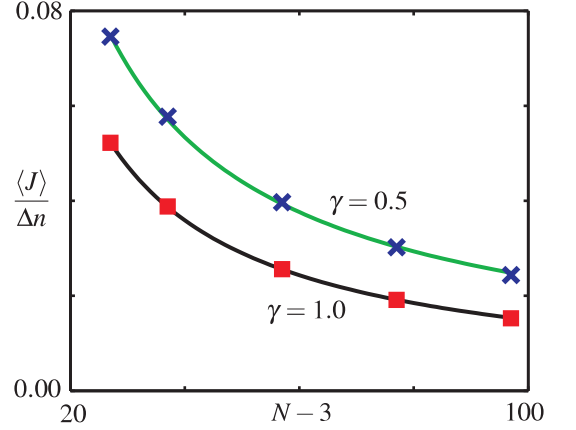


FIG. 5: The current $\langle J \rangle$ at $f = 1$, divided by the resulting density difference Δn between the ends of the system (excluding the boundary), is plotted against the system size $N - 3$ up to $N = 100$ sites. The data is for dephasing rates $\gamma = 0.5$ (\times) and $\gamma = 1.0$ (\blacksquare). The solid lines show the fitting to $\langle J \rangle / \Delta n = \kappa(N - 3)^{-\alpha}$ for each γ . These yield $\kappa = 1.288$ and $\alpha = 0.863$ for $\gamma = 0.5$, and $\kappa = 1.228$ and $\alpha = 0.958$ for $\gamma = 1.0$.

EXISTENCE OF AN APPROXIMATE DARK-STATE AT $f = 1$ WHEN $|\Delta| \gg 1$

Formally a dark-state $|\psi\rangle$ of an open quantum system is a pure state which is simultaneously an eigenstate of the Hamiltonian $H|\psi\rangle = E|\psi\rangle$ and a zero-eigenvalue eigenstate of all the jump operators comprising the dissipator $\mathcal{L}(|\psi\rangle\langle\psi|) = 0$ describing noise acting on the system. Here we show that deep in the strongly-interacting limit $|\Delta| \gg 1$, with fully polarised driving $f = 1$ as shown in Fig. 6(a), there exists a state $|\Psi_D\rangle$ which, as the system size N grows, becomes exponentially close to satisfying these requirements and is thus an approximate dark state.

In the extreme $|\Delta| \rightarrow \infty$ limit configuration states such as $|10110\dots011\rangle$, where the particle occupancy on each site of the chain is explicitly specified, are exact eigenstates of H . A key property of boundary driving is that for any value of f , it only incoherently connects configurations within a quadruplet of states $|0\mathbf{x}0\rangle, |0\mathbf{x}1\rangle, |1\mathbf{x}0\rangle, |1\mathbf{x}1\rangle$, where \mathbf{x} is any length $N - 2$ occupancy bit string. Thus, if \mathbf{x} has $(n - 1)$ 1's then the driving couples states within the total number sectors $n - 1, n$, and $n + 1$. This structure constrains the evolution caused by the driving processes to shuffling population between states in these isolated quadruplets. As depicted in Fig. 6(b), at $f = 1$ within each quadruplet, defined by \mathbf{x} , there is one configuration $|1\mathbf{x}0\rangle$ which, owing to the occupancy on the left and empty site on the right, is entirely decoupled from the driving, while also being the sink for all driving transitions. As a result the effect of this incoherent evolution alone is to eventually drive all the population among the quadruplet of states into this *dark-configuration*.

Of particular relevance here are the dark-configurations

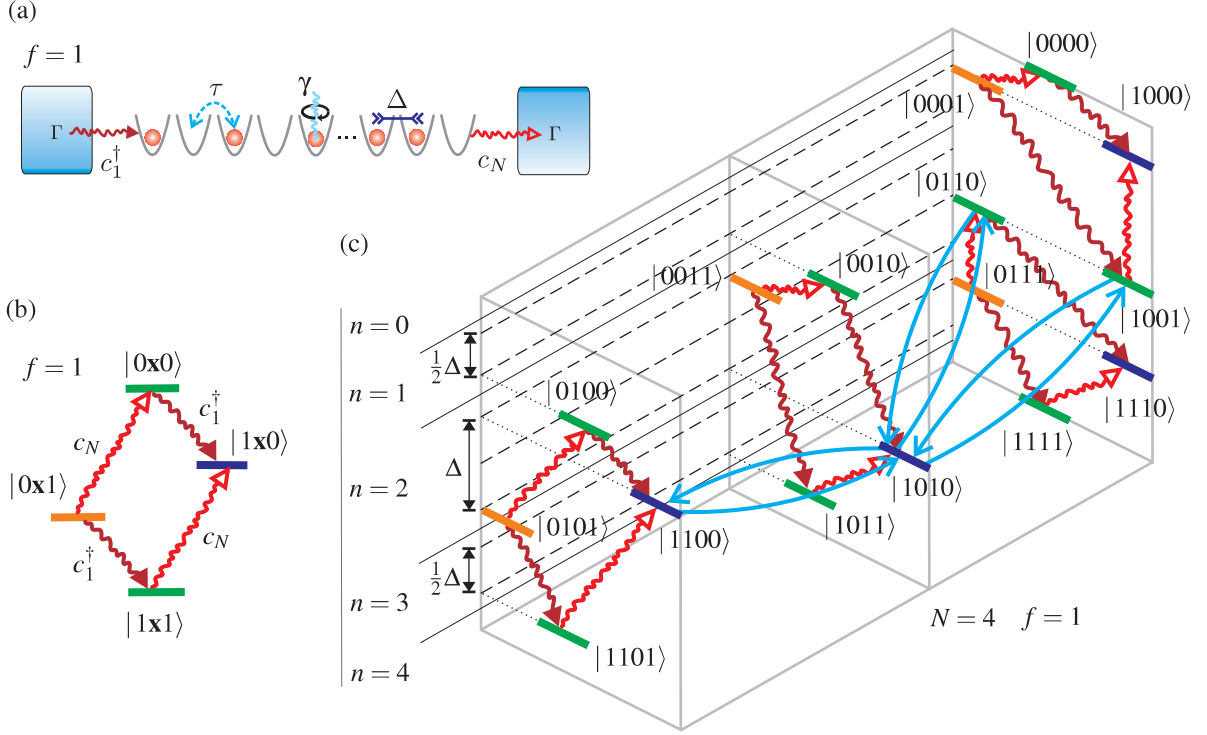


FIG. 6: (a) A schematic of the system, showing the coherent hopping τ , the nearest-neighbour density-density interaction Δ , dephasing γ , and the incoherent boundary driving in the strong driving limit $f = 1$ where the bias is maximal. In this case the driving pumps particles into the system at site 1 and ejects them at site N , both at a rate Γ . (b) For any f the driving alone incoherently connects a quadruplet of configurations $|0x0\rangle, |0x1\rangle, |1x0\rangle, |1x1\rangle$. The situation for $f = 1$ is shown where the driving can be seen to only pump into the so-called dark configuration $|1x0\rangle$. (c) For $N = 4$ sites and $f = 1$ the complete set of driving quadraplets and the transitions induced by coherent hopping between them from the half-filled domain state $|1100\rangle$ is shown. The vertical axis displays the particle number sectors and energy gaps between configurations. We observe that for $N = 4$ one hop connects $|1100\rangle$ to $|1010\rangle$, which is a dark configuration of its quadruplet, and a further hop is needed before it is coherently connected to a configuration that is not dark to the $f = 1$ driving. This disconnection between the half-filled domain configuration and the driving only occurs for $N \geq 4$, and so this is the smallest size which displays NDC.

possessing an n particle domain pinned to the left boundary as

$$|B_n\rangle = |\underbrace{111 \cdots 111}_{n} \underbrace{000 \cdots 000}_{N-n}\rangle. \quad (3)$$

For each particle number sector n the configuration $|B_n\rangle$ is separated from other relevant configurations by an energy gap $O(|\Delta|)$, akin to a domain binding energy. As we move to the limit $|\Delta| \gg 1$, hopping between configuration states occurs resulting in $|B_n\rangle$ giving rise to an eigenstate $|\Psi_D(n)\rangle$. In Fig. 7(a) the exact spectrum for $N = 12$ chain with $\Delta = 10$ is shown. For each number sector n the spectrum displays a sequence of narrow bands, split by the small finite hopping, and separated by gaps of order Δ . The highest lying eigenstate $|\Psi_D(n)\rangle$ for each sector is also highlighted. Its properties are readily determined by treating hopping as a perturbation. Specifically, to lowest-order in $[2\Delta]^{-1}$ hopping hybridizes, across an energy gap of Δ , the state $|B_n\rangle$ with the configuration $|111 \cdots 110100 \cdots 000\rangle$, where the outermost particle of the domain has broken away. In Fig. 6(c) the pattern of incoherent driving transitions and coherent hopping for $N = 4$ is

illustrated. We note that in this case $|B_2\rangle = |1100\rangle$ has no direct coherent transition to any configurations which couples to the $f = 1$ driving. More generally, so long as $N \geq 4$ and $n \geq 2$ we observe that the break-away configuration for a domain state $|B_n\rangle$ is also a dark configuration of its own quadruplet.

This approach can be taken further by computing higher-order corrections due to hopping. Since $|\Delta| \gg 1$ it is instructive to do this approximately by focusing on states of the form

$$|n, j, k\rangle = c_j c_k^\dagger |B_n\rangle, \quad (4)$$

where $1 \leq j \leq n$ and $n < k \leq N$, which describe a single break-away particle or hole propagating from the domain wall. Since the repeated action of hopping on $|B_n\rangle$ originates around the domain wall, and is also detuned by the gap Δ , we find that hopping mixes in configurations where the particle and/or hole have hopped x times in total, with an amplitude scaling as $O([2\Delta]^{-x})$. This indicates that the particle/hole propagation is suppressed with its distance from the domain wall through the unit-filled/empty regions. For each n , the eigenstate $|\Psi_D(n)\rangle$ is therefore predicted by the particle-hole picture to have a domain wall that remains exponentially localized at site n , within

a length scale $\xi \sim 1/\ln(|2\Delta|)$ [29], and a deviation $\delta_n(j)$ from the perfect domain configuration $|B_n\rangle$ given by

$$\delta_n^{\text{ph}}(j) = \begin{cases} \left(\frac{1}{|2\Delta|}\right)^{2(n-j+1)}, & 1 \leq j \leq n \\ \left(\frac{1}{|2\Delta|}\right)^{2(j-n)}, & n < j \leq N \end{cases}. \quad (5)$$

The validity of this picture is established by comparing this to the actual density deviation $\delta_n(j)$ of the exact eigenstate $|\Psi_D(n)\rangle$. In Fig. 7(b) this is done for $|\Psi_D(N/2)\rangle$ with $N = 12$, and the agreement between $\delta_n(j)$ and $\delta_n^{\text{ph}}(j)$ is seen to be excellent everywhere but the boundaries.

Since hopping predominately connects $|B_n\rangle$ with dark-configurations of the form $|1x0\rangle$, the leading order contribution to the amplitude in $|\Psi_D(n)\rangle$ for a configuration which is not dark is $O(|\Delta|^{-\min(n, |n-N/2|)})$. This corresponds to whether the hole or particle has the shortest path to the left or right boundary, respectively. In the $|\Delta| \gg 1$ limit we therefore conclude that the eigenstates $|\Psi_D(n)\rangle$, with $0 \leq n \leq N/2$, form a hierarchy of states with n , characterised by a decreasing amplitude for any configuration coupling to the $f = 1$ boundary driving. Eigenstates $|\Psi_D(n)\rangle$ with a domain size n scaling with N thus become exponentially close to being zero eigenstates of the $f = 1$ driving with increasing system size. Of these states the one with $n = N/2$, where the domain spans exactly half the chain, has the most suppressed coupling $O(|\Delta|^{-N/2})$ to the driving and is thus the closest approximation of all of them to an exact dark state.

Next, we examine the expected structure of the non-equilibrium stationary state (NESS) ρ in the $|\Delta| \gg 1$ limit. The open dynamics of particle number conserving systems like that considered here have been studied extensively [29, 37] with regard to their ergodic and mixing properties establishing that a unique NESS exists for any f . The key property ensuring this is that for a finite hopping amplitude every configuration within each particle number sector can be reached from any other, while the incoherent ejection/injection of particles by the driving connects neighbouring sectors. As a result the complete state space of the system can be accessed. Furthermore, the NESS for this open system will be block diagonal in the number sectors. At $f = 1$ the approximate dark states $|\Psi_D(n)\rangle$ for each sector n are expected to play a prominent role due to their ability to trap population. This can be better understood by approximating the NESS as a statistical mixture with probabilities p_n of these eigenstates in each sector as

$$\rho = \sum_{n=0}^N p_n |\Psi_D(n)\rangle \langle \Psi_D(n)|. \quad (6)$$

The purity of the NESS in this approximation, $\text{tr}(\rho^2) = \sum_{n=0}^N p_n^2$, is reduced only through mixing between sectors. The probabilities p_n are then determined by demanding that at stationarity there is detailed balance condition between the incoherent transition rates connecting neighbouring number sectors (see inset of Fig. 8). For sector n , as-

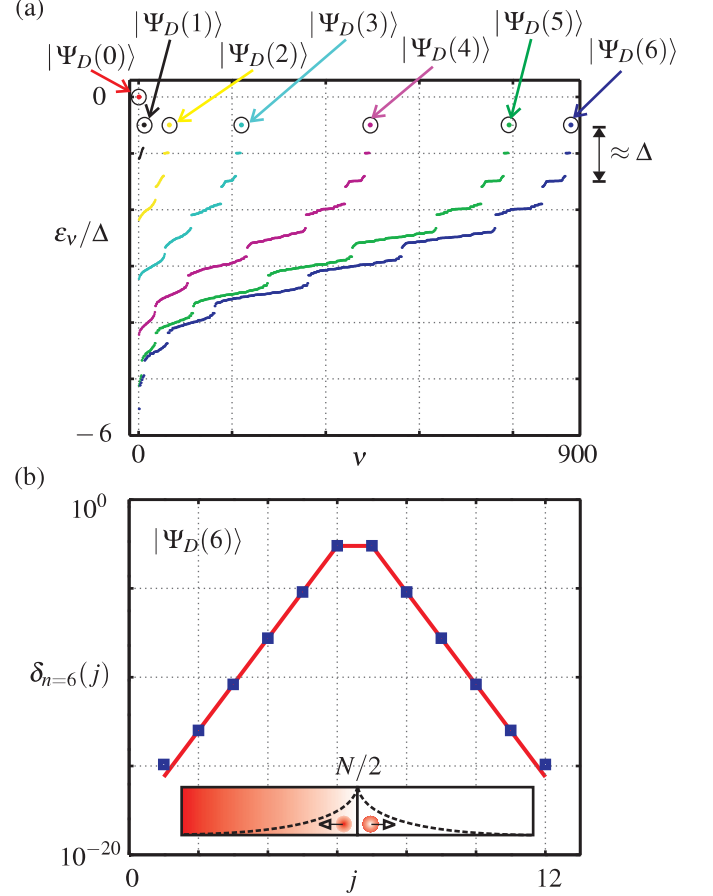


FIG. 7: (a) The energy eigen-spectrum of the spinless fermion Hamiltonian governing the chain for $N = 12$ and $\Delta = 10$. Energies ϵ_v have been shifted by $\frac{1}{4}\Delta(N-1)$ so that the state $|\Psi_D(0)\rangle = |00\dots 00\rangle$ has zero energy. The spectrum includes contributions from all particle number sectors $n = 0, \dots, 12$ with each composed of sequences of narrow bands, split by the small finite hopping, and separated by gaps of order Δ (since the spectra arising from $n = 0, \dots, 5$ are identical to those of $n = 7, \dots, 12$, only the former are shown in addition to $n = 6$). The highest lying eigenstate for each sector $|\Psi_D(n)\rangle$ is highlighted and seen to be isolated by a gap Δ from eigenstates composed of breakaway configurations $|n, i, j\rangle$. (b) For the eigenstate $|\Psi_D(6)\rangle$ the exact density deviation $\delta_n(j)$ from the corresponding boundary domain configuration $|B_n\rangle$ is shown (■), along with $\delta_n^{\text{ph}}(j)$ predicted by considering single particle/hole propagation (solid line). The inset shows a schematic of the expected exponential localization of the domain wall.

sumed to be frozen in the state $|\Psi_D(n)\rangle$, the output transition rates scale with the probability of a hole being at the left boundary as $\Gamma\langle\Psi_D(n)|c_1c_1^\dagger|\Psi_D(n)\rangle \sim \Gamma|2\Delta|^{-2n}$, and the probability of a particle being at the right boundary as $\Gamma\langle\Psi_D(n)|c_N^\dagger c_N|\Psi_D(n)\rangle \sim \Gamma|2\Delta|^{-2(N-n)}$. Considering sectors $n-1, n$ and $n+1$ we then have the equality of incoming

and outgoing transitions in n as

$$p_n \left[\left(\frac{1}{|2\Delta|} \right)^{2n} + \left(\frac{1}{|2\Delta|} \right)^{2(N-n)} \right] = p_{n-1} \left(\frac{1}{|2\Delta|} \right)^{2(n-1)} + p_{n+1} \left(\frac{1}{|2\Delta|} \right)^{2(N-n-1)}. \quad (7)$$

These equations are solved inwards from the extremal $n = 0$ and $n = N$ sectors, where $|\Psi_D(0)\rangle = |00\dots 00\rangle$ and $|\Psi_D(N)\rangle = |11\dots 11\rangle$, to give

$$p_n = p \left(\frac{1}{|2\Delta|} \right)^{2|n-N/2|^2}, \quad (8)$$

for $n = 0, 1, \dots, N$ and where $p = p_{N/2}$ is fixed by the normalization condition $\sum_{n=0}^N p_n = 1$. In Fig. 8(a) these predicted probabilities of occupation for each sector n are plotted against the exact values for the NESS with $N = 6$ and $\Delta = 10$, and found to yield excellent agreement aside from the extremal sectors. Owing to the hierarchy of approximate dark states this indicates that the NESS will be predominately a mixture of $|\Psi_D(n)\rangle$ peaked around the “best” dark state with $n = N/2$. This result also predicts that the purity of ρ scales as

$$\text{tr}(\rho^2) = 1 - \frac{1}{|\Delta|^2} + \dots, \quad (9)$$

independent of N . In Fig. 8(b) this prediction is plotted against the exact value of $1 - \text{tr}(\rho^2)$ of the NESS for $N = 6$ as a function of Δ , again showing excellent agreement even as $\Delta \rightarrow 1$.

While the discussion of the driven interacting system considered has revolved mainly around its NESS properties, the existence of approximate dark states at $f = 1$ will also heavily influence its dynamical behaviour far from stationarity. In particular, if we envisage starting at time $t = 0$ in with an empty chain, since the growth of a domain requires the propagation of holes toward the left boundaries, the increasing suppression of this process in each sector n implies that the convergence to the NESS will be exponentially slow. This is the physical reason why our numerical calculation of the NESS for $f = 1$ is limited to $N = 16$. Indeed effective suppression of the current sets in once a small domain, $n \approx 5$ has formed [29]. As a result dephasing enhancement, identical to that seen here in the NESS, equally applies to transient dynamical states where the domain has not yet saturated at $n = N/2$.

THE TOY-MODEL

The analysis so far has focused on $|\Delta| \gg 1$ and $f = 1$. In this case we saw that numerous approximate dark states, whose occupation is favoured by $f = 1$ boundary driving, cause the stationary state to become insulating. Remaining in the strongly interacting limit we now wish to isolate the effects on the transport for all drivings f , i.e. the current

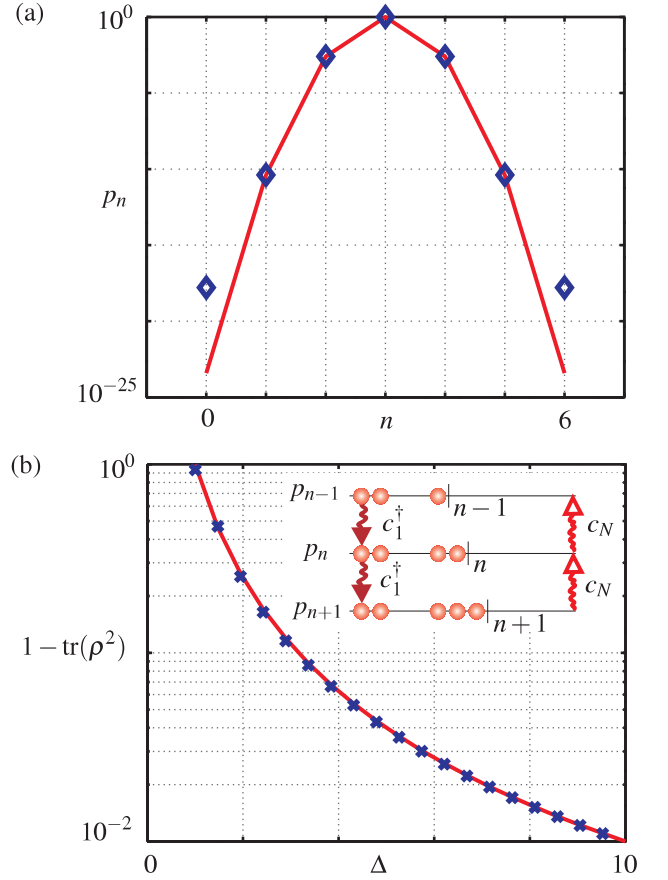


FIG. 8: (a) The probability p_n on a logarithmic scale of the NESS ρ occupying the n particle sector is shown for an exact calculation (\diamond) for $N = 6$ and the predicted form (solid line) given in Eq. (8). (b) The purity $1 - \text{tr}(\rho^2)$ against Δ of the NESS ρ on a logarithmic scale for an exact calculation (\times) for $N = 6$ and the predicted form (solid line) given in Eq. (9). The inset shows a schematic of the detailed balance approximation applied to compute these predictions.

driving profile, due to the existence of such bound states. To do so we construct a simple toy model capturing the essential physics. The structure of the model is motivated by considering the half-filled domain state $|B_{N/2}\rangle$ and its corresponding break-away configurations $|N/2, i, j\rangle$ which eventually connect it to the boundary driving. As such the toy model is composed of K configuration states $|1\rangle, |2\rangle, \dots, |K\rangle$ for some size $K > 2$. To mimic the interaction binding energy of $|B_{N/2}\rangle$, we distinguish the configuration $|K\rangle$ by elevating it in energy by Δ above the set of otherwise degenerate configurations $|1\rangle, |2\rangle, \dots, |K-1\rangle$ which model the break-away states $|N/2, i, j\rangle$. In addition to these configuration energies, the state $|1\rangle, |2\rangle, \dots, |K\rangle$ are also coherently coupled to their neighbours via “hopping” processes given by

$$H_t = \frac{1}{2} \sum_{k=1}^{K-1} (|k\rangle \langle k+1| + \text{h.c.}).$$

The current operator for the model then follows as

$$J = -i \sum_{k=1}^{K-1} (|k\rangle \langle k+1| - \text{h.c.}),$$

which measures the flow within the coherently connected configurations $|1\rangle, |2\rangle, \dots, |K\rangle$. To model the driving in the full system, which incoherently connects one particle number sector to another, we introduce an auxiliary state $|s\rangle$ whose function is simply to be an intermediary. The jump operators describing the driving then take the form

$$L_L^\pm = \sqrt{\Gamma(1 \mp f)/2} \Lambda_L^\pm, \quad L_R^\pm = \sqrt{\Gamma(1 \pm f)/2} \Lambda_R^\pm,$$

where $\Lambda_L^- = |s\rangle \langle 1|$ and $\Lambda_R^- = |K\rangle \langle s|$, with $\Lambda_L^+ = (\Lambda_L^-)^\dagger$ and $\Lambda_R^+ = (\Lambda_R^-)^\dagger$. Thus, via $|s\rangle$, the driving incoherently induces transitions between the boundary configurations $|1\rangle$ and $|K\rangle$ with a bias f . At $f = 0$ driving in both directions is equal and it is easily confirmed that the NESS is $\rho = \mathbb{1}/(K+1)$, yielding $\langle J \rangle = 0$ as in the full spinless fermion chain. At the opposite limit, $f = 1$, population is asymmetrically driven from $|1\rangle \rightarrow |K\rangle$. To complete the analogy with the full system the toy model also includes dephasing, at a rate γ , via the jump operator $L_Z = \sqrt{\gamma} \Lambda_Z$ where

$$\Lambda_Z = \mathbb{1} - 2|K\rangle \langle K|,$$

whose action is to scramble the phase of any superpositions between $|K\rangle$ and the other configurations. A schematic of the toy model illustrating all the coherent and incoherent contributions is shown in Fig. 9(a).

The current $\langle J \rangle = \text{tr}(J\rho)$ for the NESS ρ can be solved analytically for the toy model as a function of f, γ and Δ , although the complete expression is lengthy. Since the model was motivated by the perturbative limit $|\Delta| \gg 1$ of the full system the physically relevant part of this result is found by keeping only the lowest order terms in Δ^{-1} . This gives

$$\langle J \rangle \approx \frac{(K-1)(8\gamma f + (1-f)f\Gamma)}{(K+1) - 2(K-2)f + (K-1)f^2} \left(\frac{1}{\Delta}\right)^2. \quad (10)$$

In Fig. 9(b) the current-driving profile $\langle J \rangle$, rescaled by Δ^2 , is plotted for $K = 20$. Two key features emerge from this result. For $\gamma = 0$ the $(1-f)f$ in the numerator of Eq. (10), which enforces zero current at the $f = 0$ and $f = 1$, causes $\langle J \rangle$ to display negative differential conductivity (NDC). Moreover, as the expansion involves only even powers of Δ^{-1} this behaviour is independent on the sign of Δ . Dephasing enhancement of the $\langle J \rangle$ is evident from the linear γ term in Eq. (10) which eventually destroys the NDC effect. However, since γ and Γ appear only linearly it indicates that this lowest order expression is also only valid for weak dephasing and driving rates. In particular the dephasing degrading behaviour expected for large γ , due to the Zeno effect, is not described by Eq. (10). The expression is also only valid for $K \geq 3$ because NDC is not seen for $K = 2$. This is similar to how NDC is only seen for $N \geq 4$ in the full system. Just like in Fig. 6(c) for the

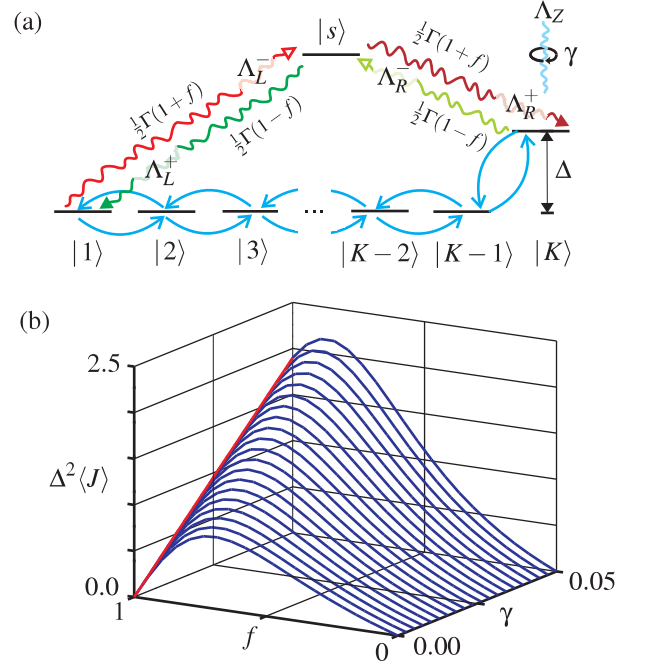


FIG. 9: (a) The schematic of the toy model and its various processes and properties. These include the nearest-neighbour coherent hopping between the set of states $|1\rangle, |2\rangle, \dots, |K\rangle$, an energy offset Δ for state $|K\rangle$, incoherent transitions $|1\rangle \leftrightarrow |s\rangle$ and $|K\rangle \leftrightarrow |s\rangle$ between the boundary states and the auxiliary state $|s\rangle$, and dephasing at a rate γ . The rates for the incoherent driving transitions $\frac{1}{2}(1 \pm f)\Gamma$ are also listed. (b) The NESS current $\langle J \rangle$, rescaled by Δ^2 , for $K = 20$, as a function of the driving f and dephasing γ , described by the approximation in Eq. (10). The behaviour at $f = 1$ with γ is emphasised by the additional (red) line.

full system, having no direct coherent coupling between the boundary configurations where driving occurs, i.e. $|1\rangle$ and $|3\rangle$ for $K = 3$, is essential for NDC to emerge. In Fig. 3(b) of the main article the exact current-driving profile for the toy model is shown for $\Delta = 2$ as a function of moderate γ 's, beyond the applicability of Eq. (10). This confirms the wider similarity of the response of the toy model to that observed in the full spinless-fermion system.

Given their similar behaviour, the toy model provides a tractable means of unravelling the origins of NDC and dephasing enhancement in the full many-body system. In Fig. 10(a) we plot the energy eigen-spectrum of the toy model. By construction we see that it mimics some of the features seen in Fig. 7(a) for a single particle number sector of the spinless fermion system. Specifically, there is a high-lying eigenstate $|\Psi_D\rangle$, separated by a gap $O(|\Delta|)$ from a dense band of eigenstates. In Fig. 10(b) this band of eigenstates are seen to be delocalized over the bulk of the system excluding the boundary configuration $|K\rangle$. For a given size K the eigenstate $|\Psi_D\rangle$ has the form $|\Psi_D\rangle \approx \sum_{k=0}^{K-1} |2\Delta|^{-k} |K-k\rangle$, to within $O(|2\Delta|^{-2K})$, as seen in Fig. 10(b). As $K \rightarrow \infty$ such an exponential wave function is simply the discrete analogue of the well known bound state of a 1D δ -potential. Given that the amplitude for

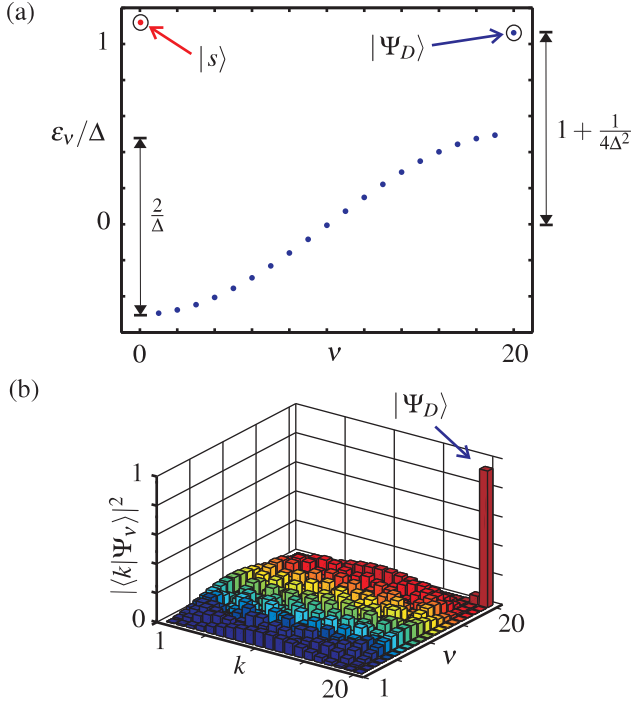


FIG. 10: (a) The spectrum ε_v of the Hamiltonian for the toy model for $K = 20$ and $\Delta = 2$. Eigenstate $v = 0$ is the highlighted auxiliary state $|s\rangle$ whose energy has been set arbitrarily. The highest-lying eigenstate $v = K$ is also highlighted and is the approximate dark-state of the model $|\Psi_D\rangle$. Beneath this state, separated by a gap $O(|\Delta|)$, is a band of eigenstates $|\Psi_v\rangle$ split by the finite hopping. (b) The probability distributions $|\langle k|\Psi_v\rangle|^2$ of the eigenstates over the configurations $|k\rangle$ are shown. The band of eigenstates are seen to be delocalized over the configurations $|1\rangle, |2\rangle, \dots, |K-1\rangle$ and expunged from the boundary configuration $|K\rangle$, while characteristic of a bound state $|\Psi_D\rangle$ is predominately peaked at $|K\rangle$ with exponential tail into bulk.

the left boundary configuration $|1\rangle$ scales as $|2\Delta|^{1-K}$, we see that $|\Psi_D\rangle$ becomes exponentially close, with increasing K , to being a dark state of the driving when $f = 1$.

The driving at $f = 1$ exclusively pumps into the configuration $|K\rangle$ whose dominant overlap is with $|\Psi_D\rangle$. Consequently so long as $\gamma = 0$ population gets progressively trapped in this dark state giving rise to $\langle J \rangle = 0$, characteristic of an insulating NESS. Remaining at $f = 1$ and switching on a non-zero dephasing directly decoheres the exponentially decaying superposition within $|\Psi_D\rangle$. This is equivalent to the coherent trapping of population, caused by the energetic gap, being bypassed by dephasing induced incoherent transitions connecting $|\Psi_D\rangle$ directly to the delocalized band of eigenstates. Current flow in the system is thus made possible via the ensuing non-stationary mixture of these eigenstates. Further increases in dephasing eventually degrades the current once the monotonically decreasing mobility of the delocalized eigenstates, caused by the Zeno effect, outweighs the flux of population escaping from $|\Psi_D\rangle$. Since the toy model only has a single

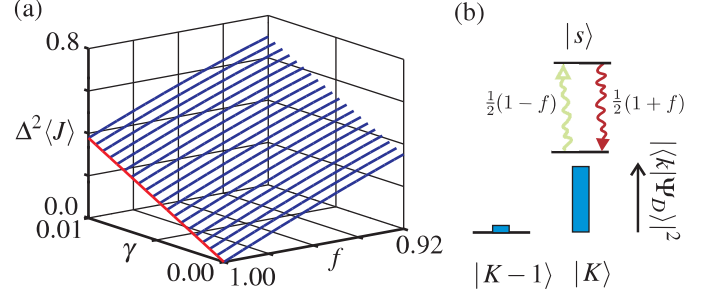


FIG. 11: (a) Identical to Fig. 9(b) the NESS current $\langle J \rangle$, rescaled by Δ^2 , for $K = 20$ is shown as a function of the driving f and dephasing γ zoomed in around the limit $f = 1$, $\gamma = 0$ insulating point. The behaviour at $f = 1$ with γ is emphasised by the additional (red) line. (b) In the strong driving limit $f \sim 1$, the Λ_R^- process $|K\rangle \rightarrow |s\rangle$ occurs at a rate $\propto (1-f) \ll 1$ making it slow (as indicated by being faded out), while the Λ_R^+ process $|s\rangle \rightarrow |K\rangle$ occurs at a rate $\propto f \approx 1$ and so is rapid. The dominant driving process is therefore $|K\rangle \rightarrow |s\rangle \rightarrow |K\rangle$, which has the effect of destroying any coherence $|K\rangle$ has with other states, such as $|K-1\rangle$.

approximate dark state $|\Psi_D\rangle$ it confirms that its existence, at one isolated point $f = 1$ and $\gamma = 0$, is alone enough to make the current-driving profile for $0 \leq f \leq 1$ and $\gamma \geq 0$ exhibit both NDC and dephasing enhancement.

Another key insight from the toy model is that the emergence of a non-zero current from the insulating point $f = 1$ and $\gamma = 0$, involves identical physics either when γ is increased slightly from zero, or when f is reduced slightly from unity. Examining Eq. (10) at $f = 1$ shows that $\langle J \rangle = 2(K-1)\gamma$, while for $\gamma = 0$ an expansion about $f = 1$ the current is $\langle J \rangle = \frac{1}{4}(K-1)(1-f)\Gamma$ to lowest order. This suggests a correspondence

$$\gamma = \frac{1}{2}(1-f)\frac{\Gamma}{4}. \quad (11)$$

which is confirmed in Fig. 11(a) in an exact calculation for $K = 20$. The equivalence is understood by considering the effect of the driving slightly below $f = 1$ where a backward flow process is introduced. In this limit the rate of driving from $|K\rangle \rightarrow |s\rangle$ taking the state out of $|\Psi_D\rangle$ is given by $\frac{1}{2}(1-f)\Gamma$ and therefore slow. In contrast the rate of driving $|s\rangle \rightarrow |K\rangle$ back is $\frac{1}{2}(1+f)\Gamma$, and therefore rapid. Focusing on the dynamics of these two driving processes alone, as in Fig. 11(b), we suppose that the initial state of the system over the configurations $|s\rangle, |K-1\rangle$ and $|K\rangle$ has the form

$$\rho(0) = \begin{pmatrix} 0 & 0 & 0 \\ 0 & \rho_{K-1}(0) & \rho_{K-1,K}(0) \\ 0 & \rho_{K-1,K}^*(0) & \rho_K(0) \end{pmatrix},$$

where there is some coherence between $|K-1\rangle$ and $|K\rangle$, but no population initially in $|s\rangle$. Evolving this state according

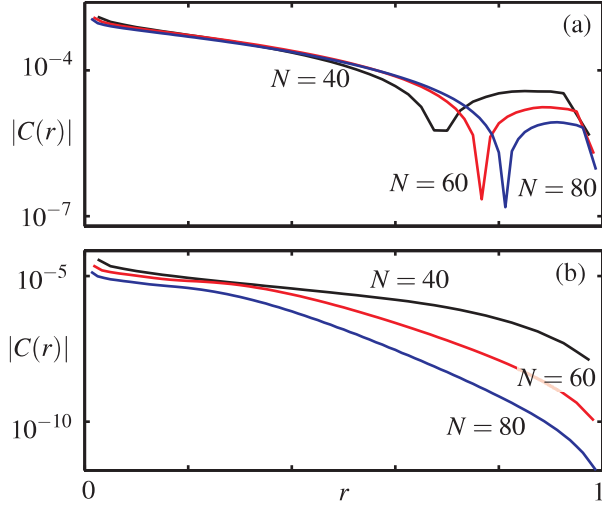


FIG. 12: The NESS density-density correlations $|C(r)|$ across the chain as a function of the fraction distance r about the centre for $\Delta = 2$ and $f = 0.1$. In (a) a moderate dephasing $\gamma = 0.05$ was included. The correlations are long-ranged and extend over a larger fraction with increasing N . This evidenced by the kink, coming from $C(r)$ changing sign, moving to larger r . In (b) a strong dephasing $\gamma = 1$ was present and the correlations are short-ranged as shown by their diminishing size and extent with increasing N .

only to these driving processes yields solutions

$$\begin{aligned}\rho_s(t) &= \frac{1}{2}(1-f)\Gamma(1-e^{-\Gamma t})\rho_K(0), \\ \rho_K(t) &= e^{-\Gamma t}\rho_K(0) + \frac{1}{2}(1+f)\Gamma(1-e^{-\Gamma t})\rho_K(0), \\ \rho_{K-1}(t) &= \rho_{K-1}(0), \\ \rho_{K-1,K}(t) &= e^{-\frac{1}{4}(1-f)\Gamma t}\rho_{K-1,K}(0).\end{aligned}$$

We therefore find that for the populations the stationary $t \rightarrow \infty$ limit is approached at a rate Γ to give $\rho_s(\infty) = \frac{1}{2}(1-f)\Gamma\rho_K(0)$ and $\rho_K(\infty) = \frac{1}{2}(1+f)\Gamma\rho_K(0)$, while the coherence $\rho_{K-1,K}(t)$ decays to zero at a rate $\frac{1}{4}(1-f)\Gamma$. Now, by considering only the dephasing process we instead find that the populations are unchanged while the coherence decays as

$$\rho_{K-1,K}(t) = e^{-2\gamma t}\rho_{K-1,K}(0).$$

Matching of these decoherence rates fits with Eq. (11). We therefore conclude that the emergence of a non-zero current when reducing f from unity is, to leading order, caused by the resulting decoherence of the dark state $|\Psi_D\rangle$, identical to

the effect of dephasing alone. This behaviour with f around $f = 1$, combined with $\langle J \rangle = 0$ at $f = 0$ and the continuity of $\langle J \rangle$ with f , is already enough to imply that NDC behaviour will be observed in the current-driving profile. Thus NDC and dephasing enhancement are underpinned by the same mechanism.

CORRELATIONS AND DEPHASING

Returning to the full spinless fermion system we now consider the effect of dephasing on two-point correlations across the chain. We find that in addition to modifying the NESS current and density profiles, dephasing also leaves a signature on the correlations which distinguishes between weakly- and strongly-interacting regimes. Specifically we compute the NESS density-density correlations $C_{ij} = \langle n_i n_j \rangle - \langle n_i \rangle \langle n_j \rangle$, where sites i and j are positioned symmetrically around the centre of the chain. This is conveniently represented as $C(r)$ where $r = |i - j|/N$ is the fractional separation of the points for the system size N , so for example $C(r = 1)$ gives the correlations between the boundaries. In Fig. 12(a) $C(r)$ is plotted for different sizes N in the strongly interacting regime with $\Delta = 2$, $f = 0.1$ and a moderate dephasing rate $\gamma = 0.05$. Finite correlations are seen to exist even for a large fractional separation r , and although they decay with r importantly these correlations are retained for a growing fraction of the chain as N increases. This property has been argued, in the $\gamma = 0$ case, to be evidence that the NESS possess genuine long-range order [32, 44]. Here our results show that this long-range order persists even in the presence of moderate dephasing, and so correlations similar to that at $\gamma = 0$ exist in the dephasing enhanced NESS. The situation for stronger dephasing $\gamma = 1$, shown in Fig. 12(b), is markedly different. Now correlations are smaller and diminish faster with r than at weaker dephasing rates. Also the correlations which are present cover a smaller fraction r (implying a fixed absolute size) as the system size N grows. The dephasing has therefore degraded the correlations to being short-ranged. Moving to the weakly interaction regime with $\Delta = 0.5$ it has previously been found [52] that correlations are short-ranged, similar in form to Fig. 12(b), even at $\gamma = 0$. Indeed a cross-over for $C(r)$ from short-ranged to long-ranged correlations at $\gamma = 0$ was found at $\Delta \gtrsim 0.91$ [52]. Like the current and density profiles, we see that also the correlations in the strongly interacting regime with large dephasing rates become increasingly similar to those of the weakly interacting regime, washing out this cross-over.